Evidence for heavy ion channeling in AlGaAs at low energies

N. G. Stoffel, S. A. Schwarz, M. A. A. Pudensi, K. Kash, L. T. Florez, J. P. Harbison, and B. J. Wilkens

Citation: Applied Physics Letters **60**, 1603 (1992); doi: 10.1063/1.107239
View online: http://dx.doi.org/10.1063/1.107239
View Table of Contents: http://scitation.aip.org/content/aip/journal/apl/60/13?ver=pdfcov
Published by the AIP Publishing

Evidence for heavy ion channeling in AlGaAs at low energies

N. G. Stoffel, S. A. Schwarz, M. A. A. Pudensi,[a] K. Kash, L. T. Florez, J. P. Harbison, and B. J. Wilkens
Bellcore, Red Bank, New Jersey 07701-7040

(Received 11 November 1991; accepted for publication 28 January 1992)

We used a new molecular dynamics simulation program to model the scattering of low-energy ions into the relatively open ⟨011⟩ axial channels of zinc-blende crystals. We also implanted 1–5 keV Si ions into GaAs/AlGaAs multiple-quantum well samples and used secondary ion mass spectrometry and photoluminescence to search for the deep ion penetration and optical damage which are characteristic of this ion channeling. Both the simulated and measured Si depth distributions have exponential tails extending at least 20 times further than the mean ion range. The photoluminescence efficiencies are severely degraded in the quantum wells which are overlapped by the observed Si profile tails. These results suggest that unintentional ion channeling is a major factor in the extensive degradation of optical and electrical properties of semiconductor surfaces which are exposed to low-energy ion bombardment during device fabrication.

Semiconductor nanostructures can be fabricated[1] with lateral dimensions of less than 100 nm using directed ion beam processes, such as reactive ion etching or chemically assisted ion beam etching. At the sub-keV ion energies used in advanced dry etching applications, most of the ion energy is deposited within 5 nm of the surface. In this layer, the defect creation rate typically has a Gaussian profile, as predicted by Monte Carlo simulation techniques[2,3] which assume no crystalline order. However, a much more extended defect profile is revealed in sensitive measurements[4–7] of low-level optical and electrical damage in crystalline targets, which often imply a distribution of defects extending tens of times deeper than the nominal ion range. It has not been conclusively demonstrated whether this deep damage is caused by radiation-enhanced diffusion of defects into the substrate or if it is produced directly by the action of energetic particles which have channeled through the open directions in the crystal lattice.

Evidence for ion channeling at sub-keV energies is found in the results of Germann *et al.*,[5] who have measured the degradation of photoluminescence (PL) efficiency in a GaAs quantum well (QW), more than 30 nm below the surface, as a function of the incidence angle of a nominal 250 eV Ar ion etching beam. In amorphous AlGaAs, an insignificant fraction of this ion beam is expected to penetrate beyond 10 nm, yet they report a dramatic decrease in PL efficiency in the QW when the Ar ions were incident within 10° of the ⟨011⟩ crystal channeling directions. There was no similar effect on the QW for ions incident along the ⟨001⟩, ⟨112⟩, or ⟨111⟩ directions. Recently,[8] we reported results of a new molecular dynamics simulation program SCHLEICH (scattering of heavy, low-energy ions into channels) which explains both the strong selectivity for ⟨011⟩ channeling and the anomalous range of the damage tails reported by Germann *et al.*[5] In most earlier studies of deep ion damage, the mass, charge state, and flux of the ion beam were not well characterized. In the present work, we study the degradation of PL efficiency in a multiple-QW (MQW) sample using a fully analyzed beam, and include a direct determination of the resulting ion profiles by high-resolution backside secondary ion mass spectrometry (SIMS).

In the SCHLEICH simulation program,[8] the sample is modeled as a semi-infinite zinc-blende lattice of atoms independently vibrating with random thermal energies. Random displacements can be applied to the atoms at the surface of the model to mimic the effects of an amorphous surface layer. This layer has uniform thickness and an abrupt interface to the perfectly crystalline lattice below. A more realistic description of the evolving structural disorder at an ion-bombarded surface would be desirable, but the channeling phenomenon is observed at a significant level in any reasonable model. The ion trajectories are calculated by integrating Hamilton's equations of motion. The instantaneous force on the ion is found by summing the repulsive electrostatic interactions (taken from the screened ZBL potential[2,3]) and the electron energy loss drag force (taken from Firsov's model[9] with empirical corrections) between the ion and all nearby lattice atoms. The lattice atoms are allowed to recoil in response to these ion-atom forces.

Wilson[10] has used SIMS to measure the profiles of 40–300 keV ^{29}Si ions implanted into GaAs along the ⟨011⟩ axis. These profiles have a distinct shoulder at the stopping depth of the most ideally channeled ions. In Fig. 1, we compare these measured channeling ranges (triangles) to SCHLEICH simulations of the average dechanneling range of ^{29}Si ions which were initially perfectly channeled along the ⟨001⟩ and ⟨011⟩ axes in an ideal GaAs lattice. Note that at medium ion energies (>10 keV), both the predicted and measured channeling ranges vary as the square root of ion energy, as expected due to the dominant contribution of electronic energy loss to the overall slowing of the ion. At lower energies, SCHLEICH predicts a range more nearly proportional to ion energy, as more energy is lost to recoil energy transfer to the lattice atoms. At still lower energies, the individual ion trajectories begin to exhibit larger excursions from the channel axis—a process which increases the

[a]Permanent address: IFGW-UNICAMP, 13081 Campinas, S. P., Brazil.

 0003-6951/92/131603-03$03.00

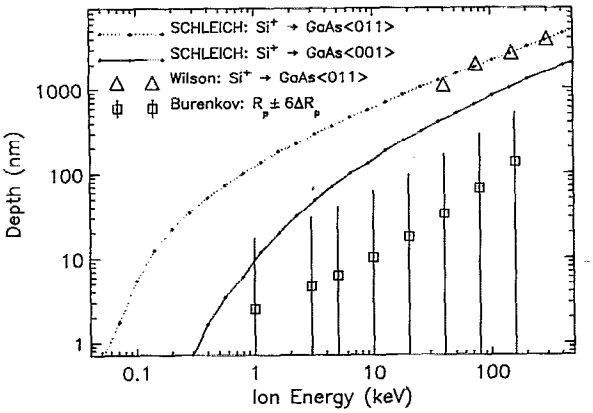

FIG. 1. Calculated average dechanneling ranges for ^{30}Si ions launched along the axes of the ⟨001⟩ or ⟨011⟩ channels in GaAs as a function of initial energy. The ion was considered to be dechanneled when the angle between its velocity and the initial axial direction was more than 16°. Wilson's data on ⟨011⟩ channeling rangs and Burenkov's estimates of nonchanneled ranges and total straggling are included for comparison.

energy loss rate and eventually leads to dechanneling and a very rapid stopping of the ion. This dechanneling process occurs at an unusually low energy in the ⟨011⟩ simulations due to dynamic effects directly related to the large aperture and high symmetry of this channel. For comparison, the mean projected ion ranges, R_p, for nonchanneled Si ions in GaAs (as tabulated by Burenkov *et al.*[11]) are plotted as squares. The vertical lines indicate the full widths of the nonchanneled ion distributions, which effectively extend beyond the mean ion range for a distance of six times the ion straggling length, ΔR_p. For low energy simulations, the only axis which shows a mean dechanneling range for Si greater than the nonchanneled ion range is the ⟨011⟩ axis. For energies less than 10 keV, where scattering cross sections are large, we find that random scattering into ⟨011⟩ directions provides the dominant contribution to deep channeling tails *regardless of the incident ion direction.*

The goal of the present work was to search for these ⟨011⟩ channeling tails. We used molecular beam epitaxy to grow a 50 nm AlAs layer on a (001) GaAs substrate followed by a 264-nm thick $Al_{0.3}Ga_{0.7}As$ film containing GaAs quantum wells of varying thickness at 50 nm intervals. The positions of the QWs were used to establish the true depth scale of the SIMS profiles presented in Fig. 2(a). In these samples, ^{29}Si and/or ^{30}Si was implanted along the [001] direction at energies of 1, 3, or 5 keV and a total fluence of 10^{15} ions cm^{-2}. The Si^+ ion beam was generated at an energy of 25 keV, mass/charge analyzed with a resolving power of 100, decelerated to the nominal implantation energy, and deflected 11° in a second magnetic analyzer to prevent any implantation of swift neutral atoms. Because the beam transport in our implanter becomes very inefficient at energies below 2 keV, we implanted $^{30}SiF_3^+$ ions at 2.9 keV to create the 1 keV sample. This molecular ion should immediately dissociate upon impact, producing a free Si ion with roughly 1 keV of kinetic energy. The samples were held at room temperature during

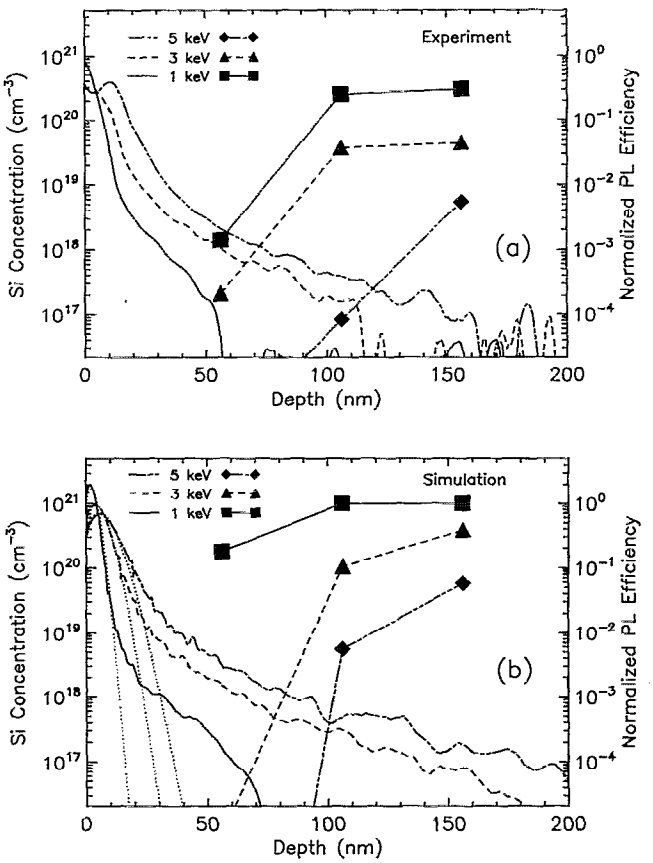

FIG. 2. (a) Silicon concentrations as recorded by SIMS for 1, 3, and 5 keV Si implantation along the [001] surface normal direction of the multiple-quantum-well sample (smoothed curves). Normalized PL efficiencies are plotted at the depth of the corresponding QW (symbols connected by straight lines for purposes of clarity). (b) Simulations of the SIMS and PL data presented in (a). The dotted curves represent the Si concentration as predicted by Burenkov's tabulated distributions for nonchanneled ions.

the implantation, and the beam power delivered to the samples was less than 1 mW cm^{-2}.

The profiles in Fig. 2(a) were measured by the backside SIMS technique,[12] as follows. Each MQW sample was heated to 110 °C for less than 5 min while a bead of black wax was melted onto the front surface. The AlAs layer which underlays the MQW layer was then dissolved by etching in room-temperature HF acid for 1–2 h. This allowed the MQW layers, supported by the wax, to be lifted off of the substrate and mounted in an ATOMIKA-3000 SIMS instrument with the bottom MQW layer facing up. Thus, the tail of Si profile due to channeling was measured in the direction from lowest to highest concentration. This minimizes the effects of forward recoil (knock-in) of Si atoms during the SIMS measurement. The SIMS profiles are distorted by charging effects within 5–15 nm of the original surface because the ion bombardment has rendered this layer nonconducting. The backside SIMS measurements are consistent with the front-side SIMS profiles (recorded on unheated samples) after accounting for the known knock-in distortion of the latter profiles. A 70 nA beam of 6 keV O_2^+ at normal incidence was used for the backside SIMS sputtering. A background signal at 29 and

30 amu, probably due to COH_x^+ fragments from the sputtering of waxy hydrocarbons, was present in all of the raw backside SIMS data, including an unimplanted sample. Therefore, a background signal on the order of 5×10^{16} cm^{-3} equivalent Si concentration has been subtracted from all profiles in Fig. 2(a).

The photoluminescence spectrum of each sample was measured at 4 K under 2 mW Ar ion laser irradiation. The QW widths were chosen so that each QW luminesced at a distinct wavelength. The areas under each PL peak in the spectrum of the virgin sample recorded. These areas were used to normalized PL yields in the ion implanted samples. Thus, we obtained the relative PL efficiencies, η, for three QWs centered at depths of 56, 106, and 156 nm, as presented in Fig. 2(a). The decrease in η from unity is roughly correlated with the local Si concentration as recorded by SIMS.

The atomic disorder at the surface of the samples was quantified using Rutherford backscattering in the channeling mode. The measured surface peak areas are equivalent to amorphous layer thicknesses of 2.0 nm in the virgin sample and 4.0, 4.5, and 5.0 nm in the 1, 3, and 5 keV implanted samples. Using these amorphous layer thicknesses, both the SIMS and PL measurements were modeled by SCHLEICH. Simulated depth profiles for ^{30}Si implanted along the [001] direction into $Al_{0.3}Ga_{0.7}As$ are shown in Fig. 2(b). As expected, most of the ions come to rest in a nearly Gaussian peak near the surface. In this region, the simulated profiles agree well with Burenkov's tabulated distributions[11] for nonchanneled ions which are plotted as dotted curves. However, roughly one percent of the ions are located in an exponential tail which extends about 20 times deeper than the peak of the Gaussian distribution. Examination of the trajectories of these deeply penetrating ions shows that they have all channeled along ⟨011⟩ directions for most of their ranges. The simulations suggest that the well-channeled ions create few vacancies until they slow to a few hundred eV, at which point they dechannel, creating a localized pocket of vacancies. Assuming a threshold energy of 15 eV for recoil displacement, SCHLEICH predicts a vacancy profile almost one order of magnitude higher than the ion profile, but with nearly identical shape.

An ion which dechannels within a quantum well can be expected to create defect centers which will sharply reduce photoluminescence over an area, A, having a radius comparable to the exciton diffusion length,[13] which is of the order of 100 nm. The normalized PL efficiency, η, can then be approximated as the fractional area of the QW which remains unperturbed after N ions have penetrated the QW per unit area; $\eta = e^{-NA} = e^{-pDA}$. Here, N is represented by the product of the ion dose, $D = 10^{15}$ cm^{-2}, and the probability, p, that an ion will dechannel in the QW, as estimated by the simulations. The value of A is used as an adjustable parameter to provide rough quantitative agreement with the measured values of η in Fig. 2(a). The symbols plotted in Fig. 2(b) show the values of η predicted for the QW sample assuming $A = 3\times10^4$ nm^2.

Note that the PL data represent a much less direct measure of the absolute number and range of the channeled ions than do the SIMS data, but provide a more direct indication of the impact of ion channeling on the electrical and optical properties of dry-etched semiconductors. Both sets of data are qualitatively reproduced within the SCHLEICH model. Within the sensitivity limits of the current experiment, it appears that SCHLEICH slightly overestimates the length of the channeling tails and the fraction of ions which channel effectively, possibly due to the simplistic treatment of surface disorder. A series of simulations were performed to study the relationship between surface disorder and channeling. If the amorphous layer thickness is varied within a reasonable range, the length scale of the channeling tail is weakly affected, but the number of ions in the tail varies more rapidly.

It might be argued that the tails observed in the SIMS profiles are the result of Si diffusion, presumably greatly enhanced by the high rate of defect creation near the bombarded surface. The greater defect creation rate at higher energies might lead to an increase in the diffusion length with energy. Note, however, that the 1 keV and 3 keV implants were performed with a 2.9 keV molecular ion beam and a 3 keV atomic ion beam, respectively, so the rates of defect production should not be sufficiently different to explain the SIMS profiles.

In conclusion, the SCHLEICH program apparently includes an adequate treatment of the scattering effects and energy loss rates for channeled ions, since these factors determine the length scale and amplitude of the observed channeling tails. Our experimental results show that ⟨011⟩ channeling is a significant and almost unavoidable phenomenon in heavy ion bombardment at energies of 1–5 keV, while our simulations suggest that channeling will occur at even lower energies. This channeling effect will produce extended defect profiles in ion-etched semiconductors even in the absence of significant defect in-diffusion.

[1] B. P. Van der Gaag and A. Scherer, Appl. Phys. Lett. **56**, 481 (1990).
[2] J. F. Ziegler, J. P. Biersack, and U. Littmark, *The Stopping and Range of Ions in Solids* (Pergamon, New York, 1985).
[3] J. P. Biersack and L. G. Haggmark, Nucl. Instrum. Methods **174**, 289 (1980).
[4] H. F. Wong, D. L. Green, T. Y. Liu, D. G. Lishan, M. Bellis, E. L. Hu, P. M. Petroff, P. O. Holtz, and J. L. Merz, J. Vac. Sci. Technol. B **6**, 1906 (1988).
[5] R. Germann, A. Forchel, M. Bresch, and H. P. Meier, J. Vac. Sci. Technol. B **7**, 1475 (1989).
[6] M. Joseph, F. E. G. Guimaraes, J. Kraus, and F. J. Tegude, J. Vac. Sci. Technol. B **9**, 1456 (1991).
[7] D. J. As, T. Frey, W. Jantz, G. Kaufel, K. Köhler, W. Rothemund, T. Schweizer, and H. P. Zappe, J. Electron. Mater. **19**, 747 (1990).
[8] N. G. Stoffel, J. Vac. Sci. Technol. (to be published).
[9] O. B. Firsov, Soviet Phys. JETP **36**, 1076 (1959).
[10] R. G. Wilson, IEEE Electron Device Lett. **3**, 210 (1982).
[11] A. F. Burenkov, F. F. Komarov, M. A. Kumakhov, and M. M. Temkin, in *Tables of Ion Implantation Spatial Distributions* (Gordon and Breach, New York, 1986), p. 371.
[12] S. A. Schwarz, C. J. Palmstrøm, C. L. Schwartz, T. Sands, L. G. Shantharama, J. P. Harbison, and L. T. Florez, J. Vac. Sci. Technol. A **8**, 2079 (1990).
[13] J. Hegarty and M. D. Sturge, J. Opt. Soc. Am. B **2**, 1143 (1985).